Supporting Information

Tungsten Phosphide Nanorod Arrays Directly Grown on Carbon Cloth: A Highly Efficient and Stable Hydrogen Evolution Cathode at All pH Values

Zonghua Pu,† Qian Liu,† Abdullah M. Asiri,§,‖ and Xuping Sun†,§,‖,*

† Chemical Synthesis and Pollution Control Key Laboratory of Sichuan Province, School of Chemistry and Chemical Engineering, China West Normal University, Nanchong 637002, Sichuan, China

§ Chemistry Department, Faculty of Science, King Abdulaziz University, Jeddah 21589, Saudi Arabia

‖ Center of Excellence for Advanced Materials Research, King Abdulaziz University, Jeddah 21589, Saudi Arabia

* Correspondence should be addressed to sun.xuping@hotmail.com (X. Sun)

EXPERIMENTAL SECTION

Materials. Red phosphorus was purchased from Aladdin Ltd. (Shanghai, China). Na_2WO_4• $2H_2O$, HCl, $(NH_4)_2SO_4$ and $H_2C_2O_4$ were bought from Beijing Chemical Corporation. CC was provided by Hongshan District, Wuhan Instrument Surgical Instruments business. All the reagents were used as received. The water used throughout all experiments was purified through a Millipore system.

Preparation of WO_3 NAs/CC and WP NAs/CC. WO_3 NAs/CC was hydrothermally prepared according to previous report.[1] Typically, 12.5 mmol of Na_2WO_4•$2H_2O$ was dissolved in deionized water (100 mL) under vigorous stirring for 30 min. Subsequently a 3 M HCl aqueous solution was slowly dropped into the solution until the pH value of the solution reached 1.2 to form a yellowish transparent solution. Then, 35 mmol $H_2C_2O_4$ was added into the above mixture and diluted to 250 mL, which resulted in the formation of the H_2WO_4 precursor. For the next step, the as-prepared 40 mL H_2WO_4 precursor was transferred into a Teflon-lined stainless autoclave (50 mL volume), and then 2 g of $(NH_4)_2SO_4$ was added to the solution. A piece of carbon cloth (1 cm×4 cm in size), which was ultrasonically cleaned by acetone, deionized water, and alcohol in sequence, was put into the autoclave and sealed, and maintained at 180 °C for 16 h. After the autoclave cooled down to room temperature, the carbon cloth was taken out and rinsed with deionized water several times and dried at 60 °C in air. The as-obtained sample was finally calcined in air at 450 °C for 1 h. For preparing WP NAs/CC, WO_3 NAs/CC and red phosphorus were put at two separate positions in a porcelain boat with red phosphorus at the upstream side of the furnace. The molar ratio for W to P is 1:5. Subsequently, the sample was heated at 800 °C for 60 min in a static Ar atmosphere, and then naturally cooled to ambient temperature under Ar. The loading for WP on CC was determined to be 2.0 mg cm^{-2} with the use of a high precision microbalance.

Characterizations. Powder XRD data were acquired on a RigakuD/MAX 2550 diffractometer with Cu Kα radiation (λ=1.5418 Å). SEM measurements were carried out on a XL30 ESEM FEG scanning electron microscope at an accelerating voltage of 20 kV. TEM measurements were performed on a HITACHI H-8100 electron

microscopy (Hitachi, Tokyo, Japan) with an accelerating voltage of 200 kV. XPS measurements were performed on an ESCALABMK II X-ray photoelectron spectrometer using Mg as the exciting source. Pressure data during electrolysis were recorded using a CEM DT-8890 Differential Air Pressure Gauge Manometer Data Logger Meter Tester with a sampling interval of 1 point per second. The generated gas was measured quantitatively using a calibrated pressure sensor to monitor the pressure change in the cathode compartment of a H-type electrolytic cell. The FE was calculated by comparing the amount of measured hydrogen generated by potentiostatic cathodic electrolysis with calculated hydrogen (assuming 100% FE). The rough agreement of both values suggests nearly 100% FE for hydrogen evolution at all pH values.

Electrochemical Measurements. Electrochemical measurements are performed with a CHI 660E electrochemical analyzer (CH Instruments, Inc., Shanghai) in a standard three-electrode system, using WP NAs/CC as the working electrode, a graphite rod as the counter electrode and a saturated calomel electrode (SCE) as the reference electrode. In all measurements, the SCE reference electrode was calibrated with respect to reversible hydrogen electrode (RHE). In 0.5 M H_2SO_4, E (RHE) = E (SCE) + 0.280 V. In 1 M PBS, E (RHE) = E (SCE) + 0.655 V. In 1 M KOH, E (RHE) = E (SCE) + 1.068 V. LSV measurements were conducted in electrolyte with scan rate of 2 mV s^{-1}. Onset overpotentials were determined based on the beginning of linear regime in the Tafel plot and iR compensation was applied for all the electrochemical measurements. A RHE potential, whose value was determined by measuring the Pt electrode's open-circuit potential once WP NAs/CC was electrochemically characterized, can be held constant by means of bubbling ~ 1 atm of research-grade H_2 into the solution.

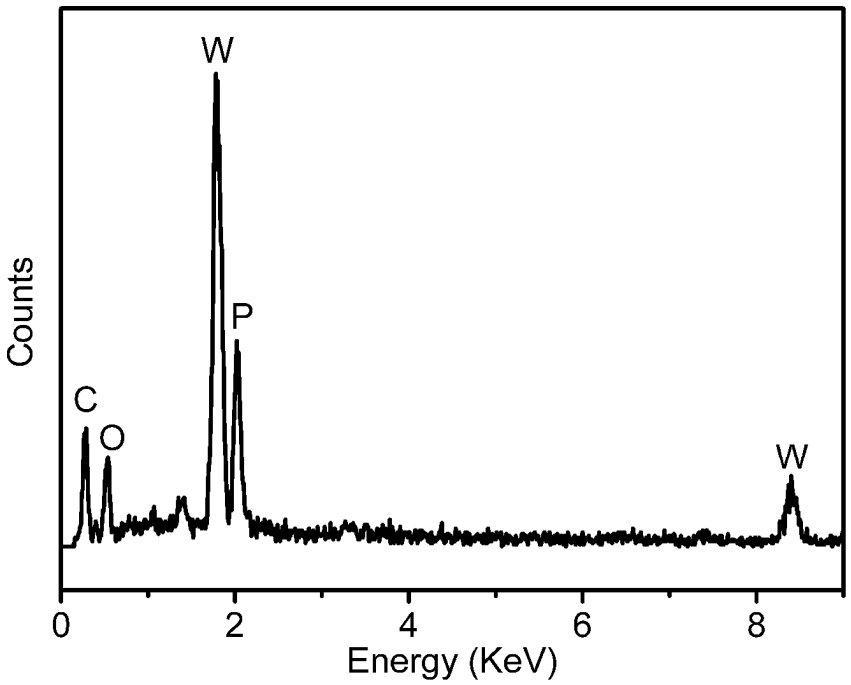

Figure S1 EDX spectrum of WP NAs/CC.

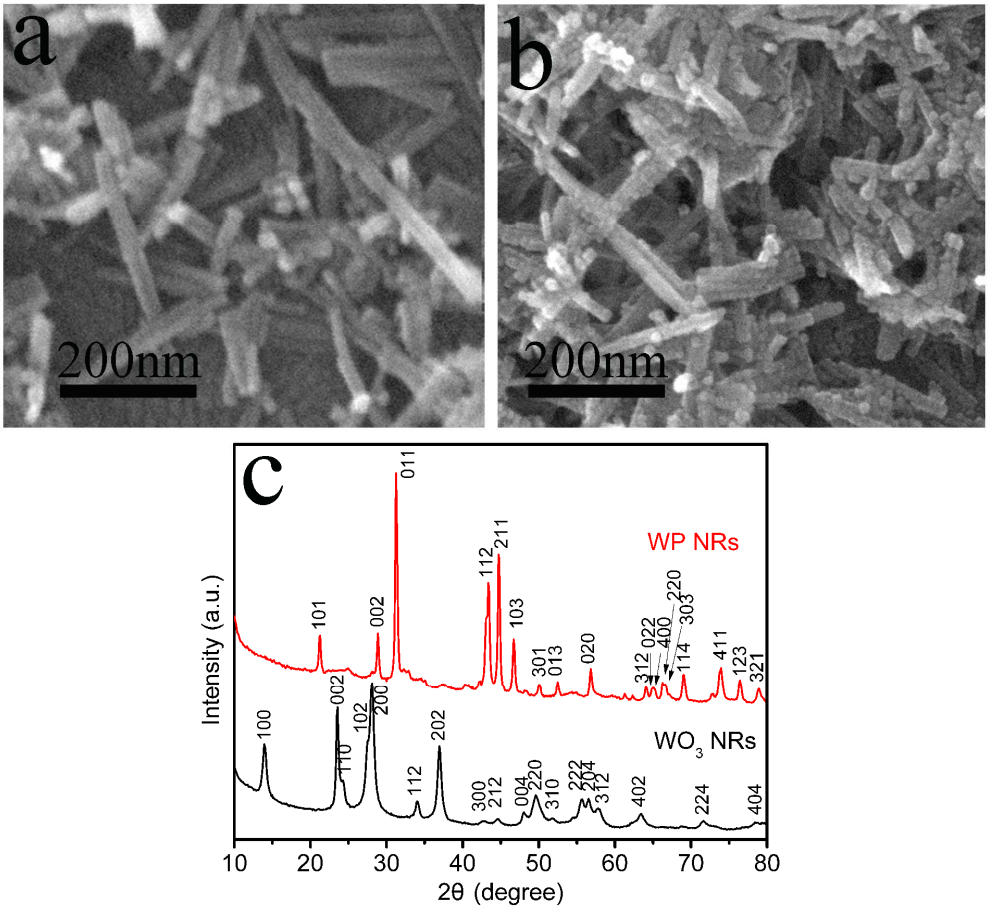

Figure S2 (a) SEM image of WO_3 NRs, (b) SEM image of WP NRs and (c) XRD patterns for WO_3 NRs and WP NRs.

Table S1 Comparison of HER performance in acid media for of WP NAs/CC with other non-noble-metal HER electrocatalysts ([a] catalysts directly grown on current collectors).

Catalyst	Onset η (mV)	Current density (j, mA cm^{-2})	η at the correspondin g j (mV)	Exchange current density (mA cm^{-2})	Ref.
$CoSe_2$ NP/CP[a]	-	10	139	$(4.9\pm1.4)\times10^{-3}$	2
double-gyroid MoS_2/FTO[a]	150-200	2	190	6.9×10^{-4}	3
metallic MoS_2 nanosheets	200	10	195	-	4
defect-rich MoS_2	120	13	200	8.9×10^{-3}	5
MoS_2/graphene/Ni foam[a]	-	10	141	-	6
MoO_3-MoS_2/FTO[a]	150-200	10	310	8.2×10^{-5}	7
bulk Mo_2C	-	1	~150	1.3×10^{-3}	8
bulk MoB	-	1	~150	1.4×10^{-3}	8
nanoporous Mo_2C nanowires	70	60	200	-	9
$NiMoN_x$/C	78	5	220	0.24	10
$Co_{0.6}Mo_{1.4}N_2$	-	10	200	0.23	11
Co-NRCNTs	50	10	260	0.01	12
exfoliated WS_2 nanosheets	80-100	10	~220	0.02	13
WS_2/graphene	150-200	10	~270	-	14
WS_2 nanoribbons	-	10	~225	-	15
WS_2 nanoflakes	100	10	~130	-	16
WS_2 nanosheets	75	10	~140	-	17
$CoSe_2$ nanobelts	50	10	~125	8.4×10^{-3}	18
Ni_2P hollow nanoparticles	-	10	116	0.033	19
Ni_2P nanoparticles	46	20	140	-	20
FeP nanosheets	100	10	~240	-	21
CoP nanoparticles	-	20	95	0.14	22
CoP/CNT	40	10	122	0.13	23
CoP/CC[a]	38	10	67	0.288	24
interconnected network of MoP nanoparticles	40	10	125	0.086	25
bulk MoP	50	30	180	0.034	26
Cu_3P NWs/CF[a]	62	10	143	0.18	27
W_2N nanorods	-	10	500	-	28
amorphous WP nanoparticles	-	10	120	-	29
WP NAs/CC[a]	50	10 100	130 230	0.29	This work

The ECSA of bare CC with GSA of 1 x 1 cm^2 was calculated using the following equation:[30]

$$i_p = 0.4463\times10^{-3}\times n^{3/2}\times F^{3/2}\times A\times C_R^*\times D_R^{1/2}\times v^{1/2}\times(RT)^{-1/2}$$

Where n is the number of electrons transferred (ferrocyanide, n=1), F is Faraday's constant (96,485 C mol^{-1}), R is the gas constant (8.314 J mol^{-1} K^{-1}), T is the temperature (298 K) and C_R^* (mol L^{-1}) is the initial ferrocyanide concentration and v is the CV scan rate (0.02 V s^{-1}). The diffusion coefficient (D_R) of ferrocyanide was based on the reference data (3.7×10^{-6} cm^2 s^{-1}). The ECSA for bare CC was calculated to be 2.0 cm^2 using CV curve shown in Figure S3a. The ECSA of the WP NAs/CC was calculated using double-layer capacitance at the solid−liquid interface with cyclic voltammogram, as shown in Figure S3b-3d. The capacitances of the double layer at the solid−liquid interface of WP NAs/CC and CC electrodes was measured by cyclic voltammograms (CVs) collected in the region of 0.20-0.30 V, where the current response should be only due to the charging of the double layer (Figure S3b-3d). The capacitance is 4.9 and 0.1 mF cm^{-2} for WP NAs/CC and bare CC, respectively.[27] Based on the ECSA of bare CC, the ECSA for WP NAs/CC was calculated to be 98.0 cm^2. Similar calculation was performed for commercial Pt/C. The ECSA of commercial Pt/C deposited on CC was 9.6 cm^2.

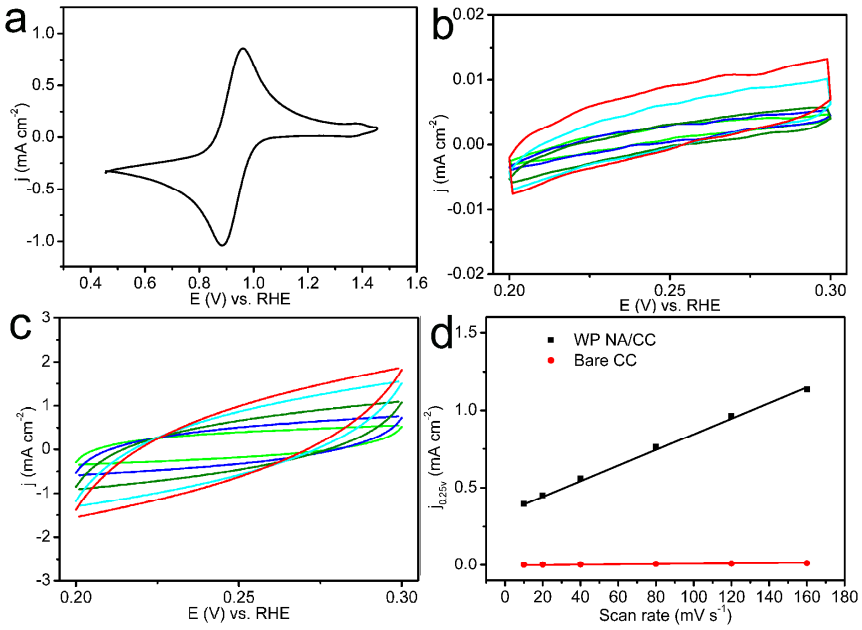

Figure S3 (a) CV of bare CC recorded at 5 mM $Fe(CN)_6^{3-/4-}$ at a scan rate of 20 mV s^{-1}. CVs for (b) bare CC and (c) WP NAs/CC. (d) The capacitive currents at 0.25 V vs. RHE as a function of scan rate for bare CC and WP NAs/CC.

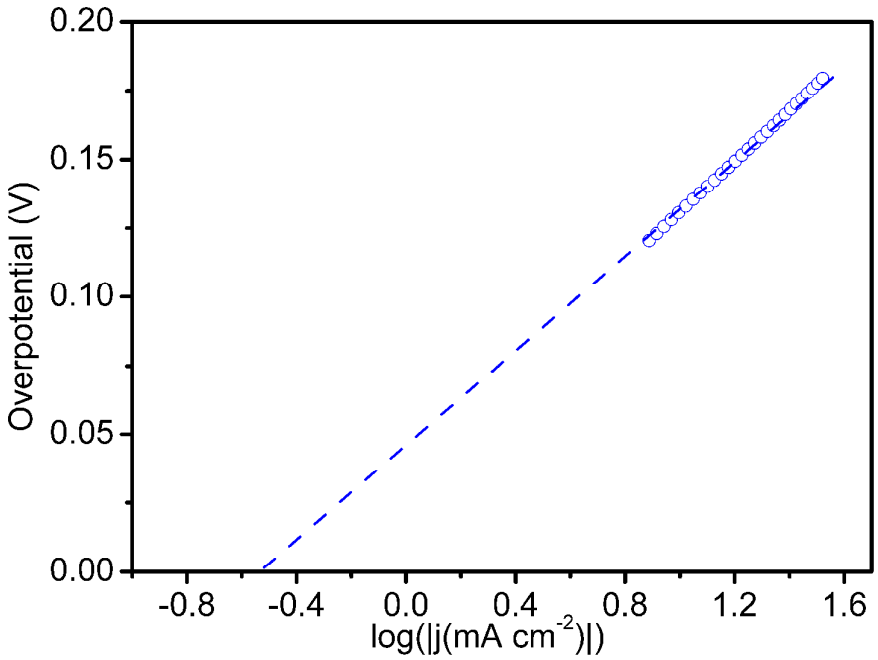

Figure S4 Calculated exchange current density of WP NAs/CC by applying extrapolation method to the Tafel plot.

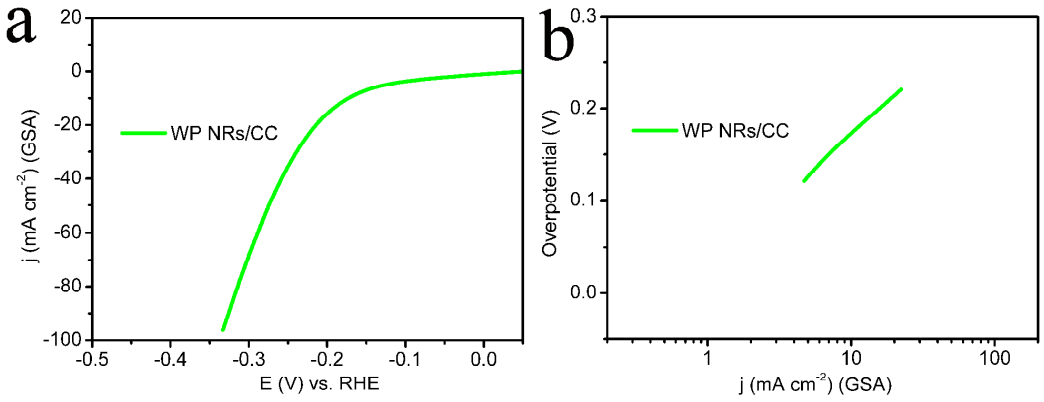

Figure S5 (a) Polarization curve for WP NRs/CC in 0.5 M H_2SO_4 with a scan rate of 2 mV s^{-1}. (b) Tafel plot for WP NRs/CC.

The number of active sites (n) was determined using cyclic voltammograms (CVs) data (Figure S6) collected between -0.2 V and +0.6 V *vs*. RHE in 1.0 M PBS solution with a scan rate of 50 mV s^{-1}. While it is difficult to assign the observed peaks to a given redox couple, n should be proportional to the integrated charge over the whole potential range. Assuming a one-electron process for both reduction and oxidation, the upper limit of n could be calculated with the following equation:

$$n = Q/2F$$

where Q is the voltammetric charge, F is Faraday constant (96500 C mol^{-1}). For WP NRs/CC, Q is 0.0136 C, n (mol) = 0.0136/(2×96500) mol = 7.04×10^{-8} mol. For WP NAs/CC, the calculated number of active site is 1.04×10^{-7}, which is nearly 1.5 times of that for WP NRs/CC.

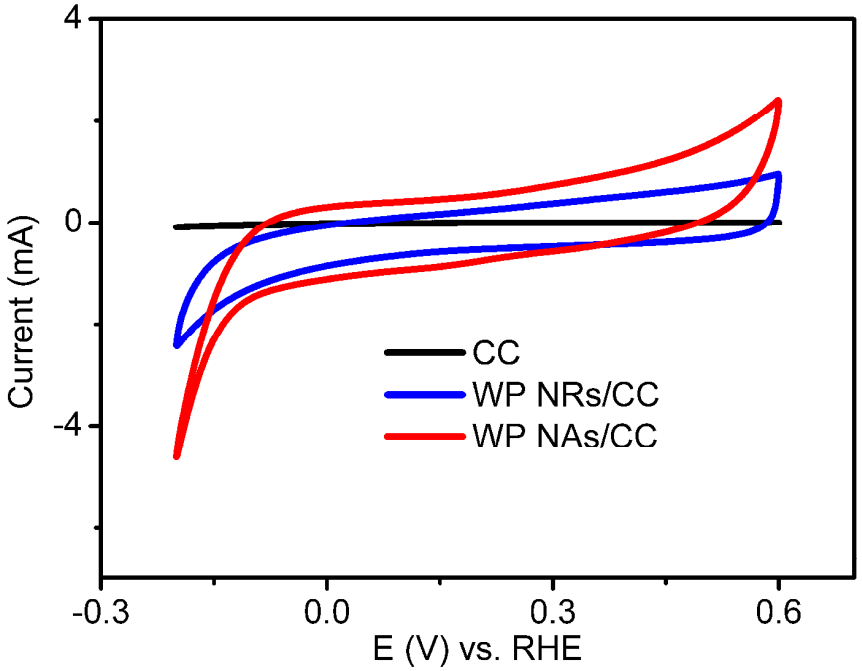

Figure S6 CVs of the CC, WP NRs/CC and WP NAs/CC recorded at 1 M PBS between -0.2 V and +0.6 V vs. RHE at a scan rate of 50 mV s^{-1}.

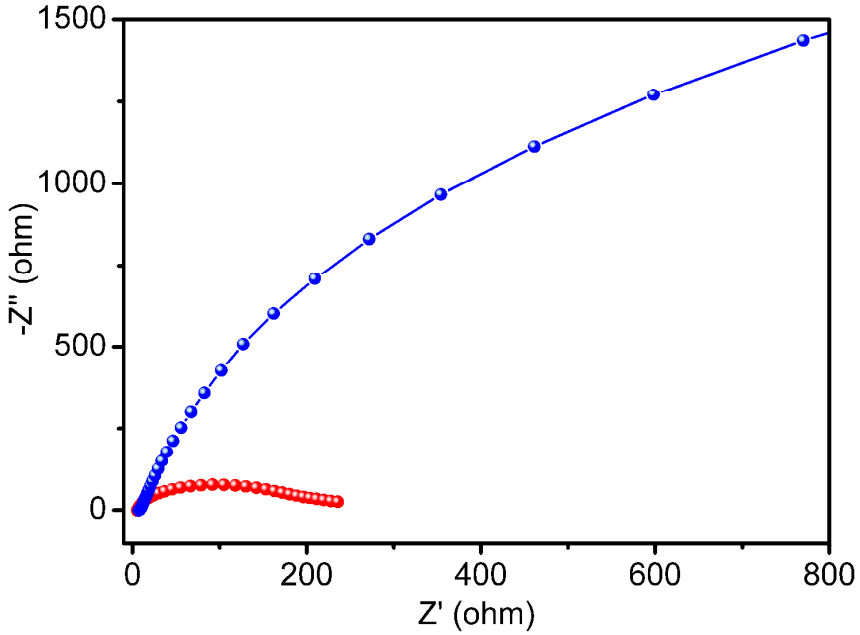

Figure S7 Nyquist plots of WP NAs/CC and WP NRs/CC recorded at 0 mV in 0.5 M H_2SO_4.

Table S2 Comparison of HER performance in neutral media for WP NAs/CC with other non-noble-metal HER electrocatalysts ([a] catalysts directly grown on current collectors).

Catalyst	Current density (j, mA cm^{-2})	Overpotential at the corresponding j (mV)	Ref.
bulk Mo_2C	1	200	8
bulk Mo_2B	1	250	8
Co-NRCNTs	2	380	12
	10	540	
CoP/CC[a]	2	65	24
H_2-CoCat/FTO[a]	2	385	31
Co-S/FTO[a]	2	83	32
$CuMoS_4$ crystals	2	210	33
WP NAs/CC[a]	2	95	This work
	10	200	

Table S3 Comparison of HER performance in alkaline media for WP NAs/CC with other non-noble-metal HER electrocatalysts ([a] catalysts directly grown on current collectors).

Catalyst	Current density (*j*, mA cm^{-2})	Overpotential at the corresponding *j* (mV)	Ref.
bulk MoB	10	225	8
Ni	10	400	8
Co-NRCNTs	1	160	12
	10	370	
CoP/CC[a]	1	115	24
	10	209	
Ni_2P nanoparticles	20	250	20
Co-S/FTO[a]	1	480	32
amorphous MoS_2/FTO[a]	10	540	34
Ni-Mo alloy/Ti foil[a]	10	80	35
Ni wire	10	350	35
WP NAs/CC[a]	10	150	This work

References

1 Gao, L.; Wang, X.; Xie, Z.; Song, W.; Wang, L.; Wu, X.; Qu, F.; Chen, D.; Shen, G. High-Performance Energy-Storage Devices Based on WO_3 Nanowire Arrays/Carbon Cloth Integrated Electrodes. *J. Mater. Chem. A* **2013**, *1*, 7167-7173.

2 Kong, D.; Wang, H.; Lu, Z.; Cui, Y. $CoSe_2$ Nanoparticles Grown on Carbon Fiber Paper: An Efficient and Stable Electrocatalyst for Hydrogen Evolution Reaction. *J. Am. Chem. Soc.* **2014**, *136*, 4897-4900.

3 Kibsgaard, J.; Chen, Z.; Reinecke, B. N.; Jaramillo, T. F. Engineering the Surface Structure of MoS_2 to Preferentially Expose Active Edge Sites for Electrocatalysis. *Nat. Mater.* **2012**, *11*, 963-969.

4 Lukowski, M. A.; Daniel, A. S.; Meng, F.; Forticaux, A.; Li, L.; Jin, S. Enhanced Hydrogen Evolution Catalysis from Chemically Exfoliated Metallic MoS_2 Nanosheets. *J. Am. Chem. Soc.* **2013**, *135*, 10274-10277.

5 Xie, J.; Zhang, H.; Li, S.; Wang, R.; Sun, X.; Zhou, M.; Zhou, J.; Lou, X.; Xie, Y. Defect-Rich MoS_2 Ultrathin Nanosheets with Additional Active Edge Sites for Enhanced Electrocatalytic Hydrogen Evolution. *Adv. Mater.* **2013**, *25*, 5807-5813.

6 Chang, Y.; Lin, C.; Chen, T.-Y.; Hsu, C.-L.; Lee, Y.-H.; Zhang, W.; Wei, K.-H.; Li, L.-J. Highly Efficient Electrocatalytic Hydrogen Production by MoS_x Grown on Graphene-Protected 3D Ni Foams. *Adv. Mater.* **2013**, *25*, 756-760.

7 Chen, Z.; Cummins, D.; Reinecke, B. N.; Clark, E.; Sunkara, M. K.; Jaramillo, T. F. Core–shell MoO_3–MoS_2 Nanowires for Hydrogen Evolution: A Functional Design for Electrocatalytic Materials. *Nano Lett.* **2011**, *11*, 4168-4175.

8 Vrubel, H.; Hu, X. Molybdenum Boride and Carbide Catalyze Hydrogen Evolution in both Acidic and Basic Solutions. *Angew. Chem. Int. Ed.* **2012**, *54*, 12703-12706.

9 Liao, L.; Wang, S.; Xiao, J.; Bian, X.; Zhang, Y.; Scanlon, M.; Hu, X.; Tang, Y.; Liu, B.; Girault b, H. A Nanoporous Molybdenum Carbide Nanowire as an Electrocatalyst for Hydrogen Evolution Reaction. *Energy Environ. Sci.* **2014**, *7*, 387-392.

10 Chen, W.; Sasaki, K.; Ma, C.; Frenkel, A. I.; Marinkovic, N.; Muckerman, J. T.; Zhu, Y.; Adzic, R. R. Hydrogen-Evolution Catalysts Based on Non-Noble Metal Nickel–Molybdenum Nitride Nanosheets. *Angew. Chem. Int. Ed.* **2012**, *51*, 6131-6135.

11 Cao, B.; Veith, G. M.; Neuefeind, J. C.; Adzic, R. R.; Khalifah, P. G. Mixed Close-Packed Cobalt Molybdenum Nitrides as Non-noble Metal Electrocatalysts for the Hydrogen Evolution Reaction. *J. Am. Chem. Soc.* **2013**, *135*, 19186-19192.

12 Zou, X.; Huang, X.; Goswami, A.; Silva, R.; Sathe, B. R.; Mikmekova, E.; Asefa, T. Cobalt-Embedded Nitrogen-Rich Carbon Nanotubes Efficiently Catalyze Hydrogen Evolution Reaction at All pH Values. *Angew. Chem. Int. Ed.* **2014**, *126*, 4372-4376.

13 Voiry, D.; Yamaguchi, H.; Li, J.; Silva, R.; Alves, D. C. B.; Fujita, T.; Chen, M.; Asefa, T.; Shenoy, V. B.; Eda, G.; Chhowalla, M. Enhanced Catalytic Activity in Strained Chemically Exfoliated WS_2 Nanosheets for Hydrogen Evolution. *Nat. Mater.* **2013**, *12*, 850-855.

14 Yang, Y.; Voiry, D.; Ahn, S. J.; Kang, D.; Kim, A. Y.; Chhowalla, M.; Shin, H. S. Two-Dimensional Hybrid Nanosheets of Tungsten Disulfide and Reduced Graphene Oxide as Catalysts for Enhanced Hydrogen Evolution. *Angew. Chem. Int. Ed.* **2013**, *52*, 13751-13754.

15 Lin, J.; Peng, Z.; Wang, G.; Zakhidov, D.; Larios, E.; Yacaman, M. J.; Tour, J. M. Enhanced Electrocatalysis for Hydrogen Evolution Reactions from WS_2 Nanoribbons. *Adv. Energy Mater.* DOI: 10.1002/aenm.201301875.

16 Cheng, L.; Huang, W.; Gong, Q.; Liu, C.; Liu, Z.; Li, Y.; Dai, H. Ultrathin WS_2 Nanoflakes as a High-Performance Electrocatalyst for the Hydrogen Evolution Reaction. *Angew. Chem. Int. Ed.* **2014***, 53*, 7860-7863.

17 Lukowski, M. A.; Daniel, A. S.; English, C. R.; Meng, F.; Forticaux, A.; Hamers. R.; Jin, S. Highly Active Hydrogen Evolution Catalysis from Metallic WS_2 Nanosheets. *Energy Environ. Sci.* **2014**, *7,* 2608-2613.

18 Xu, Y.; Gao, M.; Zheng, Y.; Jiang, J.; Yu, S. Nickel/Nickel(II) Oxide Nanoparticles Anchored on Cobalt(IV) Diselenide Nanobelts for Electrochemical Hydrogen Production. *Angew. Chem. Int. Ed.* **2013**, *52*, 8546-8550.

19 Popczun, E.J.; McKone, J R.; Read, C. G.; Biacchi, A. J.; Wiltrout, A. M.; Lewis, N. S.; Schaak, R. E. Nanostructured Nickel Phosphide as an Electrocatalyst for the Hydrogen Evolution Reaction. *J. Am. Chem. Soc.* **2013**, *135*, 9267-9270.

20 Feng, L.; Vrubel, H.; Bensimon, M.; Hu, X. Easily-Prepared Dinickel Phosphide (Ni_2P) Nanoparticles as an Efficient and Robust Electrocatalyst for Hydrogen Evolution. *Phys. Chem. Chem. Phys.* **2014**, *16*, 5917-5921.

21 Xu, Y.; Wu, R.; Zhang, J.; Shi, Y.; Zhang, B. Anion-Exchange Synthesis of Nanoporous FeP Nanosheets as Electrocatalysts for Hydrogen Evolution Reaction. *Chem. Commun.* **2013**, *49*, 6656-6658.

22 Popczun, E. J.; Read1, C. G.; Roske, C. W.; Lewis, N. S.; Schaak, R. E. Highly Active Electrocatalysis of the Hydrogen Evolution Reaction by Cobalt Phosphide Nanoparticles. *Angew. Chem. Int. Ed.* **2014**, *53*, 5427-5430.

23 Liu, Q.; Tian, J.; Cui, W.; Jiang, P.; Cheng, N.; Asiri, A. M.; Sun, X. Carbon Nanotubes Decorated with CoP Nanocrystals: A Highly Active Non-Noble-Metal Nanohybrid Electrocatalyst for Hydrogen Evolution. *Angew. Chem. Int. Ed.* **2014**, *53*, 6710-6714.

24 Tian, J.; Liu, Q.; Asiri, A. M.; Sun, X. Self-Supported Nanoporous Cobalt Phosphide Nanowires Array: An Efficient 3D Hydrogen-Evolving Cathode Over the Wide Range 0-14 pH. *J. Am. Chem. Soc.* **2014**, *136*, 7587-7590.

25 Xing, Z.; Liu, Q.; Asiri, A. M.; Sun, X. Closely Interconnected Network of Molybdenum Phosphide Nanoparticles: A Highly Efficient Electrocatalyst for Generating Hydrogen from Water. *Adv. Mater.* **2014**, *26*, 5702-5707.

26 Xiao, P.; Sk, M. A.; Thia, L; Ge, X.; Lim, R. J.; Wang, J.; Lim, K. H.; Wang, X. Molybdenum Phosphide as an Efficient Electrocatalyst for the Hydrogen Evolution Reaction. *Energy Environ. Sci.* **2014**, *7*, 2624-2629.

27 Tian, J.; Liu, Q.; Cheng, N.; Asiri, A. M. Sun, X. Self-Supported Cu_3P Nanowires Array as an Integrated High-Performance 3D Cathode for Generating Hydrogen from Water. *Angew. Chem. Int. Ed.* **2014**, *53*, 9577-9581.

28 Chakrapani, V.; Thangala, J.; Sunkara, M. K. WO_3 and W_2N Nanowire Arrays for Photoelectrochemical Hydrogen Production. *Int. J. Hydrogen Energy* **2009**, *34*, 9050-9059.

29 McEnaneya, J. M.; Cromptonb, J. C.; Callejasa, J. F.; Popczuna, E. J.; Reada, C. G.; Lewis, N. S.; Schaak, R. E. Electrocatalytic Hydrogen Evolution Using Amorphous Tungsten Phosphide Nanoparticles. *Chem. Commun.* **2014**, *50*, 11026-11028.

30 Zhao, Y.; Nakamura, R.; Kamiya, K.; Nakanishi, S.; Hashimoto, K. Nitrogen-doped Carbon Nanomaterials as Non-metal Electrocatalysts for Water Oxidation. *Nat. Commun.* **2013**, *4*, 2390-2397.

31 Cobo, S.; Heidkamp, J.; Jacques, P.-A.; Fize, J.; Fourmond, V.; Guetaz, L.; Jousselme, B.; Ivanova, V.; Dau, H.; Palacin, S.; Fontecave, M.; Artero, V. A Janus Cobalt-based Catalytic Material for Electro-splitting of Water. *Nat. Mater.* **2012**, *11*, 802-807.

32 Sun, Y.; Chong, L.; Grauer, D.; Yano, J.; Long, J.; Yang, P.; Chang, C. Electrodeposited Cobalt-Sulfide Catalyst for Electrochemical and Photoelectrochemical Hydrogen Generation from Water. *J. Am. Chem. Soc.* **2013**, *135*, 17699-17702.

33 Tran, P.; Nguyen, M.; Pramana, S.; Bhattacharjee, A.; Chiam, S.; Fize, J.; Field, M.; Artero, V.; Wong, L.; Loo, J.; Barber, J. Copper Molybdenum Sulfide: A New Efficient Electrocatalyst for Hydrogen Production from Water. *Energy Environ. Sci.* **2012**, 5, 8912-8916.

34 Merki, D.; Fierro, S.; Vrubel, H.; Hu, X. Amorphous Molybdenum Sulfide Films as Catalysts for Electrochemical Hydrogen Production in Water. *Chem. Sci.* **2011**, *2*, 1262-1267.

35 McKone, J.; Sadtler, B.; Werlang, C.; Lewis, N.; Gray, H. Ni–Mo Nanopowders for Efficient Electrochemical Hydrogen Evolution. *ACS Catal.* **2013**, *3*, 166-169.